

Chromophore Selectivity and Tuning in a Far-Red/Red Cyanobacteriochrome

Manuel Mora, Marcus V. Moreno, Nathan C. Rockwell and J. Clark Lagarias

McNair Scholar's Journal

May 2019

ABSTRACT

Cyanobacteriochromes (CBCRs) are linear tetrapyrrole (bilin) chromophore based, bi-stable light-sensing photoreceptors in the phytochrome superfamily that exhibit spectral diversity ranging from the near-UV to the far red. CBCRs detect specific wavelengths of light and elicit responses including phototaxis and light acclimation. The growing field of optogenetics uses light sensing proteins to control intracellular processes in cells, tissues and whole organisms. However, optogenetic applications in live mammals are limited by poor tissue penetrance of short wavelengths of light to which most available probes respond. Optogenetic probes tuned to respond to far-red wavelengths are thus desirable for less invasive optogenetic applications in whole animals. The recently discovered CBCR JSC1_58120g3 from *Leptolyngbya* sp. JSC-1 exhibits a far-red/red photocycle that senses light in the near infrared 'window' of tissue penetrance. JSC1_58120g3 senses far-red light due to its atypical 18¹-18² dihydrobiliverdin (DHBV) chromophore instead of the phycobilin chromophore precursor, phycocyanobilin (PCB). Although mammals do not synthesize phycobilins, they do produce biliverdin IX α (BV), a chromophore precursor that can substitute for DHBV in JSC1_58120g3. In this work, we have exploited unpublished X-ray crystal structures of JSC1_58120g3 and sequence alignments to closely related CBCRs to identify conserved residues that we hypothesize are involved in the unusual bilin selectivity of this CBCR. Through targeted mutagenesis, we have identified a single proline residue that is essential for verdin specificity. Preliminary analysis of additional mutants affecting other conserved positions has thus far been inconclusive.

INTRODUCTION

Many organisms utilize photosensitive proteins to derive information from the light environment. Light sensing in this context is a separate mechanism from photosynthesis, in which organisms harvest light as a form of energy. The evolution of non-photosynthetic photoreceptors has enabled many organisms to adapt to their light environment, *e.g.* for regulating more effective photosynthetic light harvesting, triggering a damage avoidance response to UV light, or phototaxis (1). The phytochrome superfamily is a diverse class of light-sensitive proteins that detect light with a covalently bound linear tetrapyrrole (bilin) chromophore buried within a highly conserved cGMP-phosphodiesterase/Adenylyl-cyclase/FhlA (GAF) domain (2). Phytochrome photocycles consist of two stable light-absorbing red (R)- and far-red (FR)-absorbing states. Like rhodopsins, light sensing is mediated by *Z*-to-*E* isomerization of a double bond in their bilin chromophore. Plant phytochromes exhibit a R/FR photocycle that regulates various responses to the ratio of R to FR light, including shade avoidance, flowering, and seed germination (3, 4).

Phytochromes are attractive targets for engineering optogenetic tools owing to their spectral overlap with the near-infrared window for optimal light penetrance into mammalian tissue (5). R/FR phytochrome signaling has been exploited to control processes including gene transcription (6) and actin assembly (7) using only light input in heterologous host organisms. However, phytochromes possess several qualities that limit their potential as optogenetic tools. First, they are FR-absorbing only in the *E* state, while the dark-adapted *Z* state responds to less tissue-penetrative R light. Therefore,

FR-mediated optogenetic responses mediated by phytochromes require R pre-illumination. Second, most phytochromes are quite large due to the requirement for three domains for light sensing activity. Compared with the much smaller (albeit blue-absorbing) LOV-domain based optogenetic tools (8), the large size of phytochrome size increases the potential for non-specific, off-target interactions.

Cyanobacteriochromes (CBCRs) are distant relatives of phytochromes that require the GAF domain alone for full photochemistry (9). Typically less than 200 amino acids, CBCRs are similar in size to LOV domains yet have achieved unparalleled spectral diversity ranging from the near-UV to the FR (9-18). Moreover, two classes of FR-sensing CBCRs have recently been described, both of which are FR-absorbing in the dark-adapted state. One class exhibits FR/R and FR/O photocycles with peak absorbances in the near infrared, i.e. 726-740 nm (17). This class of FR-sensors, like most CBCRs, only accepts phycobilin chromophore precursors like PCB. PCB is only produced by photosynthetic organisms via a two-step, four electron reduction of BV (Figure 1) (19). The second class exhibits FR/O photocycles. Although this class is less FR-shifted at 697-713 nm, it can incorporate BV as chromophore precursor (20, 21). Since BV is widely produced in most organisms as a product of heme degradation, this class is better suited for mammalian applications.

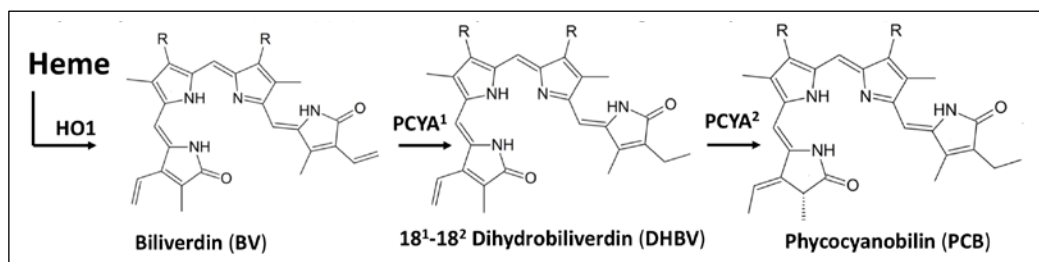


Figure 1 - Biosynthesis of PCB from Heme. Heme is converted to biliverdin IX α (BV) by a heme oxygenase. BV is further reduced to phycocyanobilin (PCB) via a two-step, four-electron reduction catalyzed by phycocyanobilin:ferredoxin oxidoreductase (PCYA) with the intermediate 18¹,18² dihydrobiliverdin (DHBV).

Recently, a third class of FR CBCRs typified by JSC1_58120g3 has been found to have FR/R photocycles with peak absorbances at 712-728 nm for the dark-adapted Z state (unpublished work). This class of CBCRs readily bind to verdin chromophore precursors including BV and the two electron-reduced 18¹,18² dihydrobiliverdin (DHBV) (Figure 1). This class also does not bind the A-ring-reduced phycobilins, despite their excess abundance in bacterial strains engineered to produce phycobilins. The high affinity for verdin precursors, together with their red-shifted photocycles makes this third class of FR CBCRs promising candidates for optogenetic applications. Moreover, JSC1_58120g3 has already been engineered into a FR/R photoactivatable adenylyl cyclase for production of cAMP (22). Understanding the mechanisms behind the red-shifted photocycle, verdin affinity, and phycobilin exclusion in these CBCRs may help to further optimize their properties for optogenetic tool development. In this study, we leverage the crystal structure of JSC1_58120g3 bound to 18¹,18² DHBV (unpublished work) along with sequence alignments of other members of this FR/R CBCR subfamily to identify conserved residues that contribute to the aforementioned properties (Table 1). We first chose to substitute these residues for those found at equivalent positions in

NpR6012g4, a PCB-binding CBCR that exhibits a R/G photocycle. By measuring the UV-vis spectra of native and denatured variants to establish their photocycles and chromophore identities, respectively, we identify Pro591 to be critical for phycobilin exclusion. Mutation of additional conserved residues has thus far been inconclusive, with several variants retaining photocycles very similar to wild-type, and others ablating or reducing chromophore binding. Further mutation of the latter by targeting Pro591 to restore phycobilin binding will be necessary to fully evaluate any effects on photocycle tuning and verdin affinity.

Table 1- Conserved residues in JSC1_58120g3

| CBCR | β 1-2 | α 3 | α 4 | β 5 | β 6 |
|--------------|-------------------------------|---------------------------------------|--|---------------------------|---------------------------|
| JSC1_58120g3 | 562 KFREDFYFGD | 590 DPYLNEH | 633 LTDCHEAL | 648 SCAVVA | 663 LLSAFQ |
| NpR_6012g4 | RFNPNWTGE | DTHLQET | HSPCHIEIL | AYVIVP | LLAAYQ |

METHODS

Variant cloning. Synthetic pUC57 plasmids were ordered from GenScript with codon optimized sequences for each JSC1_58120g3 mutant described in Table 2. The synthetic genes were excised from pUC57 using NcoI and XmaI restriction enzymes (NEB) and ligated into ampicillin-resistant arabinose-inducible pBAD (Invitrogen) plasmid using T4 DNA ligase (NEB) following manufacturer protocols.

Table 2 – JSC1_58120g3 variants characterized in this study.

| Mutant ID | Point Mutations (JSC1_58120 numbering) |
|------------------------------|---|
| 58120g3- β 1 | K562R, R564N, D570E |
| 58120g3- β 2 | Y567W, F568S |
| 58120g3- β 1 β 2 | K562R, R564N, Y567W, F568S, D570E |
| 58120g3- α 4 | L633H, T634S |
| 58120g3- β 5 | C649Y, V651I, A653P |
| 58120g3- β 6 | S665A, F667Y |
| 58120g3- β 5 β 6 | C649Y, V651I, A653P, S665A, F667Y |
| Full RG 58120g3 | K562R, R564N, Y567W, F568S, D570E, P591T, Y592H, N594Q, H596T, L633H, T634S, A640I, C649Y, V651I, A653P, S665A, F667Y |

Mutagenesis. To acquire P591T and A640I mutants, a pBAD plasmid containing wild-type JSC1_58120g3 with in-frame intein-chitin binding domain tag was modified via site-directed mutagenesis. HPLC-purified mutagenic primers (Table 3) were ordered from

Invitrogen Custom Primers. Reactions were assembled with Pfu Ultra DNA polymerase (Agilent), Pfu Ultra buffer, pBAD-JSC1_58120g3 plasmid, primers, and dNTP mix (Invitrogen) according to manufacturer instructions. Samples were cycled in an Applied Biosystems 2720 thermal cycler (Table 4). PCR products were digested with DpnI and heat shock-transformed into chemically competent XL-1 E. coli. Plasmid DNA was purified using the QIAprep Spin Miniprep kit (QIAGEN), and sequences confirmed by Sanger Sequencing (Quintara).

Table 3 – Primers for JSC1_58120g3 mutagenic PCR

| Target Mutation | Primer Forward Sequence | Primer Reverse Sequence |
|-----------------|--|---|
| P591T | 5'CAGCGGTTGGGAAGACcC GTA CTTGAACGAACA 3' | 5'TGTTTCGTTCAAGTACGgGTC TTCCCAACCGCTG 3' |
| A640I | 5'AACCGATTGCCACATTGAAa tCTTGGAATCCTTCGAGGTG 3' | 5'CACCTCGAAGGATTCCAAGa tTTCAATGTGGCAATCGGTT 3' |

Table 4- PCR cycle utilized for the site-directed mutagenesis; A640I and P591T

| | Initial Denaturation | 30 Cycles | | | Final Extension | Cooldown |
|--------------|----------------------|-----------|-------|-------------|-----------------|----------|
| Temp. | 95 °C | 95 °C | 55 °C | 68 °C | 68 °C | 4 °C |
| Time | 30 sec | 30 sec | 1 min | 1.25 min/kb | 10 min | ∞ |

Expression and Purification. Mutant plasmids were transformed into chemically competent kanamycin resistant strain LMG194 engineered to produce PCB under IPTG induction. Transformants were grown for five hours at 37 °C with 220 RPM shaking in 100 mL RM media with 25 µg/mL kanamycin and 50 µg/mL ampicillin. These cultures were transferred into 1L LB media containing 25 µg/mL kanamycin, 50 µg/mL ampicillin, and 1 mM IPTG at 37 °C. After 1 hour shaking at 220 RPM, arabinose was added to 0.002% w/v, followed by another hour of shaking at 37 °C before the temperature was lowered to 20 °C and shaken overnight. Cultures were centrifuged at 5,000 g to pellet cells, which were then frozen at -80 °C until purification. Frozen cells were thawed and resuspended in Lysis Buffer (20 mM HEPES pH 8.0, 500 mM NaCl, 1 mM EDTA, 0.1% v/v Triton X-100), lysed using a microfluidizer, and centrifuged at 35,000 rpm for 30 min prior to loading onto a 3 cm x 3 cm chitin column (NEB) that was pre-washed with 10 volumes of Lysis Buffer and pre-equilibrated at 4 °C. After sample application, the resin was washed with 10 volumes of Wash Buffer (20 mM HEPES pH 8.0, 500 mM NaCl, 1 mM EDTA), and loaded with 2 volumes of Cleavage Buffer (20 mM HEPES pH 8.0, 500 mM NaCl, 1 mM EDTA, 50 mM DTT) for overnight incubation to initiate cleavage of the intein-CBD tag. The subsequently eluted protein was dialyzed 3 hours at 4 °C in 1L TKKG buffer (25 mM TES-K pH 8.0, 25 mM KCl, 10% glycerol), followed by overnight dialysis at 4 °C in fresh 1L TKKG buffer.

Spectroscopic Measurements. Purified proteins were analyzed with a Cary 50 spectrophotometer modified for illumination from above with a 75 W xenon source

equipped with bandpass filters used for triggering photochemistry (670 +/- 40 nm, 650 +/- 40 nm, and 550 +/- 70 nm). A far-red LED (Sanyo) peaking at 728 nm was used to trigger FR photochemistry. For denaturation assays, 100 μ L of protein was added to 1 mL of 7 M guanidinium chloride containing 1% (v/v) HCl. White light illumination of denatured samples was performed using the xenon lamp filtered through a 320 nm long-pass filter.

RESULTS

A conserved proline residue is necessary for PCB exclusion. Pro591 and Ala640 of JSC1_58120g3 are conserved in other closely related FR CBCRs all of which appear to exclude PCB chromophore precursor in favor of DHBV (unpublished work). Comparison of the crystal structures of JSC1_58120g3 with the structure of the red/green (R/G) CBCR AnPixJg2 reveals that these residues afford a 1 \AA narrower binding pocket around the chromophore A-ring than the equivalent Thr292 and Ile325 residues present in AnPixJg2 (Figure 2).

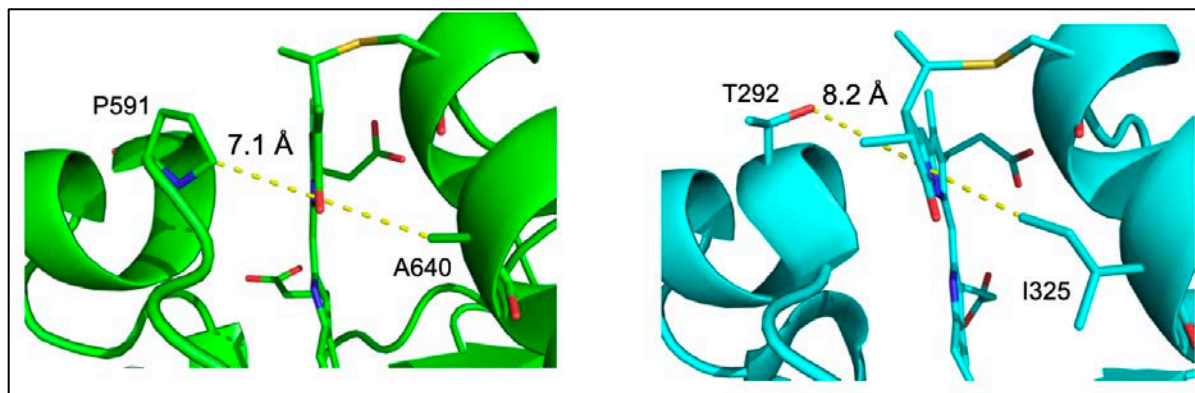


Figure 2- A mechanism for phycobilin exclusion. Left, CBCR JSC1_58120g3 bound to DHBV is shown colored by atom type (green, carbon; blue, nitrogen; red, oxygen; yellow, sulfur). The residues Pro591 and Ala640 form a 7.1 \AA wide binding pocket at the chromophore A-ring. Right, CBCR AnPixJg2 (3W2Z) bound to PCB is shown colored by atom (cyan, carbon; blue, nitrogen; red, oxygen; yellow, sulfur). The residues Thr292 and I325 form a wider 8.2 \AA binding pocket at the chromophore A-ring.

Based on this evidence, we reasoned that the narrower DHBV binding pocket bounded by Pro591 and Ala640 might provide the structural basis for excluding PCB chromophore due to its bulky tetrahedral geometry at C2 and C3 of the A-ring. By contrast, DHBV with its trigonal planar geometry and less steric bulk at the equivalent positions would be better accommodated. Indeed, substitution of proline for threonine (P591T) was able to restore PCB binding, resulting in a red/orange (R/O) photocycle with peaks at 662 nm and 612 nm (Figure 3B; Table 5). A small FR shoulder suggests that this variant may still bind DHBV (Figure 3B). Denaturation analysis of P591T was in good agreement with denatured NpR6012g4, a standard for incorporation of PCB chromophore (Figure 3F; Table 5). By comparison, the A640I mutant retained a photocycle similar to WT JSC1_58120g3 (Figure 3C). The P591T A640I double mutant exhibited similar properties to the P591T single mutant, albeit with incomplete forward photochemistry (Figure 3D). Taken together, these data show that Pro591 is critical for

exclusion of phycobilin chromophore precursors with reduced A-rings but that both large and small residues at position 640 do not affect the ability to exclude phycobilins. In addition, the presence of a FR shoulder and red-shifted Z- and E-states imply that as yet un-identified mechanisms can influence verdin affinity and chromophore tuning in JSC1_58120g3.

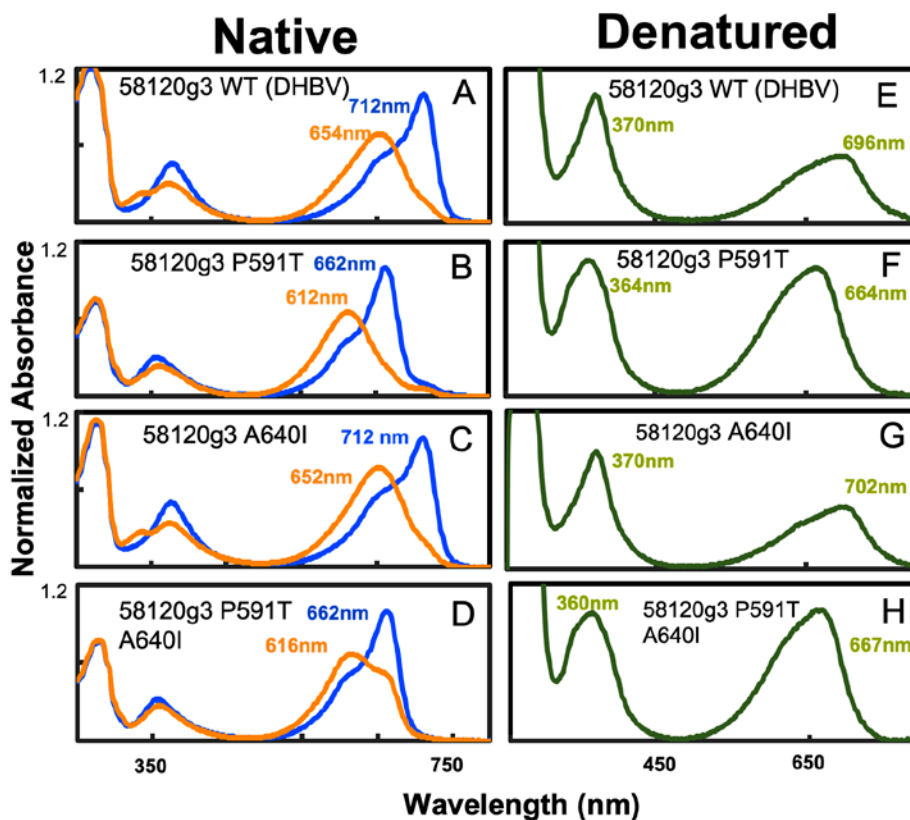


Figure 3 – UV-vis spectra of phycobilin exclusion variants of JSC1_58120g3. (A-D) Dark-adapted 15Z (blue) and photoproduct 15E (orange) absorption spectra are shown for WT JSC1_58120g3 (A), P591T (B), A640I (C), and P591T A640I (D) mutants. (E-H) Denatured 15Z absorption spectra are shown for WT JSC1_58120g3 (E), P591T (F), A640I (G), and P591T A640I (H) mutants.

Variants of JSC1_58120g3 with reduced chromophore incorporation. Residues in the $\beta 5$ and $\alpha 4$ regions have been shown to be important for BV affinity in other types of CBCRs (18), and conserved residues in these regions (Table 1) are located near the chromophore. We therefore introduced substitutions of the residues in these regions (Table 2) to determine whether they affect verdin affinity in JSC1_58120g3. Unfortunately, $\beta 5$ - and $-\beta 5\beta 6$ variants exhibited complete loss of covalent chromophore attachment (Table 5). It therefore is not clear if this reflects specific loss of verdin binding or loss of any chromophore to bind, due to protein misfolding or to altered non-covalent binding orientation to preclude covalent attachment. The 58120g3- $\alpha 4$ variant was able to attach DHBV chromophore precursor to produce an adduct with a FR/R photocycle similar to WT JSC1_58120g3 (Figure 4A; Table 5). However, 58120g3- $\alpha 4$ exhibited a markedly lower specific absorbance ratio (SAR), indicative of reduced DHBV incorporation efficiency (Table 5). Interestingly, the 58120g3- $\beta 6$ variant with conserved residues located near the chromophore D-ring also exhibited a notably reduced SAR compared to the wild type (Figure 4B; Table 5). This may indicate that the $\beta 6$ region

plays a role in verdin affinity in JSC1_58120g3, in contrast to other BV-binding CBCRs. Finally, 58130g3- β 1 β 2 had a similarly reduced SAR (Figure 4C; Table 5), although the altered residues in this variant do not appear close to the chromophore but instead are likely to disrupt several electrostatic interactions. To distinguish variants affecting verdin affinity from those with poor protein folding or generally diminished chromophore affinity, it will be necessary to restore phycobilin binding.

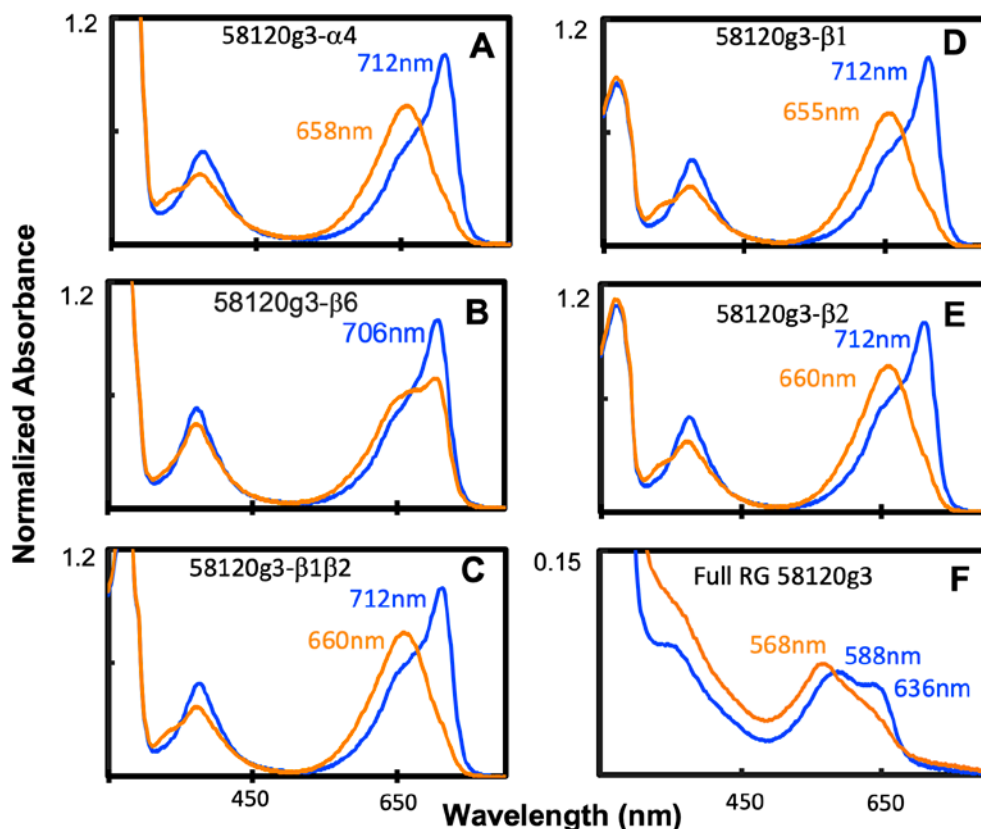


Figure 4 – UV-vis spectra of JSC1_58120g3 variants. Dark-adapted 15Z (blue) and photoproduct 15E (orange) absorption spectra are shown for 58120g3- α 4 (A), 58120g3- β 6 (B), 58120g3- β 1 β 2 (C), 58120g3- β 1 (D), 58120g3- β 2 (E), and Full RG (F) variants.

Additional mutations with minimal changes to FR/R DHBV photocycle. The conserved residues located on strands β 1 and β 2 in JSC1_58120g3 form a network of electrostatic interactions with residues surrounding helix α 3. R/G CBCRs including NpR6012g4 and slr1393g3 do not possess these interactions, and upon photoconversion have been observed to undergo substantial rearrangement in this region, with the PCB-adduct A-ring twisting towards helix α 3. We therefore surmised that the electrostatic interactions contributed by the β 1 and β 2 conserved residues could serve to rigidize this region in JSC1_58120g3, thereby preventing A-ring twist upon photoconversion and substantially red-shifting photoproduct absorption. However, 58120g3- β 1, - β 2, and - β 1 β 2 variants each exhibited very similar photocycles to wt-JSC1_58120g3 with DHBV-adduct (Figure 4C-E; Table 5). Indeed, none of the JSC1_58120g3 variants tested herein displayed substantial alteration to *E*-state peak absorption, and only the 58120g3- β 6 variant exhibited a notable blue shift in *Z*-state absorption (Table 5).

Table 5 – Spectral parameters of JSC1_58120g3 variants

| CBCR | Chromophore | Native Z/E peak (nm) | Denatured Z peak (nm) | SAR ^a |
|------------------------------|-------------|----------------------|-----------------------|------------------|
| NpR6012g4 (WT) | PCB | 652/542 | 662 | 0.98 |
| 58120g3 P591T | PCB | 662/612 | 664 | 1.36 |
| 58120g3 A640I | DHBV | 712/652 | 702 | 0.90 |
| 58120g3 P591T, A640I | PCB | 662/616 | 666 | 1.31 |
| JSC1_58120g3 (WT) | DHBV | 712/654 | 696 | 0.91 |
| 58120g3_β1 | DHBV | 712/656 | 702 | 1.26 |
| 58120g3_β2 | DHBV | 712/660 | 700 | 0.95 |
| 58120g3_β1β2 | DHBV | 712/660 | 698 | 0.79 |
| 58120g3_α4 | DHBV | 710/658 | 700 | 0.44 |
| 58120g3_β5 | none | N/A | N/A | N/A |
| 58120g3_β6 | DHBV | 706/unclear | 698 | 0.78 |
| 58120g3_β5 β6 | none | N/A | N/A | N/A |
| Full RG 58120g3 ^b | PCB | 636/568 | 664 | N/A |

^aSpecific absorbance ratio (SAR) calculated as ratio of absorbance at peak Z wavelength to absorbance at 280 nm

^bFull RG 58120g3 was unstable and aggregated during data collection, and exhibited multiple peaks. Peak wavelengths are estimates.

An unstable light sensor after complete substitution of conserved residues. To probe for potential cooperative effects of conserved positions, we fully substituted JSC1_58120g3 conserved residues with the equivalent residues found in the R/G CBCR NpR6012g4 (Tables 1 and 2). The resulting protein was highly unstable, with short-wavelength scatter build-up over time indicative of protein aggregation. Despite its instability, the Full-RG variant bound to PCB chromophore and exhibited multiple peaks in each photostate (Figure 4F; Table 5), perhaps representing inactive chromophore sub-populations. These factors make Z/E peak wavelengths difficult to assign, although it exhibits 636 nm and 588 nm Z-state peaks, and an E-state peak at 568 nm. These wavelengths are notably blue shifted in both photostates relative to the R/O photocycle observed with P591T, indicating that the red-shifting mechanism of JSC1_58120g3 may depend on a combination of conserved residues that we have yet to test.

DISCUSSION

Through our mutagenic studies with the FR CBCR JSC1_58120g3, we have identified a conserved proline residue that is necessary for the exclusion of chromophore precursors with a reduced A-ring such as PCB. Through mutagenesis of this residue, we were able to restore the ability to incorporate PCB. Together with crystal structures of JSC1_58120g3 showing that this proline narrows the binding pocket around the chromophore A-ring, our studies provide substantial insight into the mechanism behind PCB exclusion. The bulky P591 near the A-ring binding pocket likely provides a steric hindrance that is sufficient to prevent incorporation of PCB, but can readily bind DHBV with its more planar A-ring geometry. The P591T variant introduced threonine; the residue present in several PCB-binding R/G CBCRs including NpR6012g4 and

AnPixJg2. This substitution also restored PCB incorporation with a R/O photocycle. The P591T *Z*-state at 662 nm is red shifted by about 10-15 nm compared to prototypical R/G CBCRs, while the *E*-state at 612 nm is red-shifted by nearly 70 nm (14). Both photostates also retain a small FR shoulder likely indicative of a minor sub-population with bound DHBV. Taken together, this indicates that P591T retains a mechanism for red-shifting both photostates, particularly for the *E*-state, while also retaining an affinity for verdin precursors. Therefore, other residues not yet identified are likely responsible for these properties in JSC1_58120g3 and closely related CBCRs.

Variants that affect the ability of JSC1_58120g3 to bind verdin chromophore also are expected to reduce chromophorylation efficiency of DHBV and BV chromophores. Several mutants fall within this category, including JSC1_58120g3- α 4 and JSC1_58120g3- β 6 which exhibit reduced SAR relative to wild-type, as well as JSC1_58120g3- β 5 and JSC1_58120g3- β 5 β 6 both of which exhibit no chromophore binding. However, these effects must be distinguished from wholesale impairment of the ability to bind any bilin precursor; for example, removing the conserved Cys required for covalent attachment of chromophore will deplete the ability to bind PCB in addition to DHBV or BV. In each of these variants, the crucial phycobilin-excluding P591 remains in place, and is likely preventing incorporation of PCB. In order to determine if the ability to incorporate PCB precursor has been affected, it is necessary to restore PCB binding through the P591T mutation in each of the diminished SAR variants. We expect that variants with reduced affinity specifically for verdin chromophores will exhibit PCB incorporation similar to that of the P591T single mutant. Notably, the full RG transition that contains mutations of all identified conserved residues including Pro591 is able to bind PCB chromophore, although the protein is unstable and denatures quickly. While not conclusive due to the number of additional mutations, this shows that in some contexts, JSC1_58120g3- α 4, - β 5, and - β 6 mutants can be compatible with a PCB chromophore. A more direct probe of the effects of these variants on verdin and phycobilin affinity will be to individually combine them with the P591T mutation.

With the exception of P591T-containing variants which bind to PCB chromophore rather than DHBV, most of the targeted mutations caused minimal shift to the *Z*- and *E*-state peak wavelengths. An explanation for the red-shifted absorbance, particularly in the *E*-state therefore remains elusive. R/G CBCRs including NpR6012g4 and slr1393g3 have been shown to induce substantial blue shift of their *E*-state peak absorption in part by twisting their PCB chromophore A- and D-rings out of plane relative to the B- and C-rings (23, 24). The “twisted” chromophore has a shortened conjugated π -electron system and therefore absorbs shorter wavelengths of light than the more extended “relaxed” conformation. Analysis of photoconversion-induced blue shift against peak *Z*-state absorption for several known CBCRs has shown that sensors with “twisted” *E*-states follow a distinct trendline that is separate from those with “relaxed” *E*-states (17). Extending this analysis to include FR CBCRs such as AM1_1557g2 and AM1_C0023g2 that are FR/O with BV-adduct but R/G with PCB-adduct reveals that they follow the “twisted” trendline when bound to PCB, but the “relaxed” trendline when bound to BV (unpublished work). Indeed, all known BV- and DHBV-adducts appear to have “relaxed” *E*-states by this analysis. This may imply that verdin chromophores are intrinsically more “relaxed” and red-shifted in the *E*-state. Therefore, it may be necessary to introduce the P591T mutation into other conserved residue variants to restore PCB

binding. If DHBV chromophore-adduct is intrinsically relaxed, it could mask any protein changes to chromophore tuning, which would only be revealed with a “twistable” PCB-adduct. Again, the full RG transition may offer some limited insight here; its *Z/E* peak wavelengths can be assigned as 636 nm/568 nm. This would make it a R/G sensor with peak wavelengths much more in line with those of typical R/G CBCRs. However, the instability of the protein coupled with multiple peaks in the *Z*- and *E*-states makes the spectra difficult to interpret. Addition of the P591T mutation to individual variants may yield more stable proteins with cleaner photocycles.

Our studies therefore reveal one crucial residue, i.e. P591, that is necessary for the unusual phycobilin exclusion observed in JSC1_58120g3 and closely related FR CBCRs. Mutation of additional conserved residues has yet to identify the mechanisms behind the photocycle red shift or the affinity for verdin chromophores, although work in these areas is ongoing. These three unusual traits make JSC1_58120g3 and related CBCRs attractive candidates for the development of optogenetic tools – in particular for mammalian applications where FR-shifted, BV-binding photoreceptors are highly sought after. Understanding the molecular basis for these traits could allow for engineering of improvements such as further FR-shifted absorbance, increased BV affinity, or transfer of BV affinity to other CBCRs (18). This will serve to expand the spectral diversity of BV-compatible CBCRs, creating a more complete toolbox of optogenetic probes that are compatible with the wide array of BV-producing organisms.

REFERENCES

1. Narikawa R, *et al.* (2011) Novel photosensory two-component system (PixA-NixB-NixC) involved in the regulation of positive and negative phototaxis of cyanobacterium *Synechocystis* sp. PCC 6803. *Plant Cell Physiol* 52(12):2214-2224.
2. Rockwell NC & Lagarias JC (2010) A brief history of phytochromes. *Chemphyschem* 11(6):1172-1180.
3. Pham VN, Kathare PK, & Huq E (2018) Phytochromes and Phytochrome Interacting Factors. *Plant Physiol* 176(2):1025-1038.
4. Bae G & Choi G (2008) Decoding of light signals by plant phytochromes and their interacting proteins. *Annu Rev Plant Biol* 59:281-311.
5. Weissleder R (2001) A clearer vision for in vivo imaging. *Nat Biotechnol* 19(4):316-317.
6. Shimizu-Sato S, Huq E, Tepperman JM, & Quail PH (2002) A light-switchable gene promoter system. *Nat Biotechnol* 20(10):1041-1044.
7. Leung DW, Otomo C, Chory J, & Rosen MK (2008) Genetically encoded photoswitching of actin assembly through the Cdc42-WASP-Arp2/3 complex pathway. *Proc Natl Acad Sci USA* 105(35):12797-12802.
8. Zimmerman SP, *et al.* (2016) Tuning the Binding Affinities and Reversion Kinetics of a Light Inducible Dimer allows control of transmembrane protein localization. *Biochemistry* 55(37):5264-5271.
9. Ikeuchi M & Ishizuka T (2008) Cyanobacteriochromes: a new superfamily of tetrapyrrole-binding photoreceptors in cyanobacteria. *Photochem Photobiol Sci* 7(10):1159-1167.

10. Ulijasz AT, *et al.* (2009) Cyanochromes are blue/green light photoreversible photoreceptors defined by a stable double cysteine linkage to a phycoviolobin-type chromophore. *J Biol Chem* 284(43):29757-29772.
11. Song J-Y, *et al.* (2011) Near-UV cyanobacteriochrome signaling system elicits negative phototaxis in the cyanobacterium *Synechocystis* sp. PCC 6803. *Proc Natl Acad Sci USA* 108(26):10780-10785.
12. Rockwell NC, Martin SS, Feoktistova K, & Lagarias JC (2011) Diverse two-cysteine photocycles in phytochromes and cyanobacteriochromes. *Proc Natl Acad Sci USA* 108(29):11854-11859.
13. Rockwell NC, Martin SS, Gulevich AG, & Lagarias JC (2012) Phycoviolobin formation and spectral tuning in the DXCF cyanobacteriochrome subfamily. *Biochemistry* 51(7):1449-1463.
14. Rockwell NC, Martin SS, & Lagarias JC (2012) Red/Green cyanobacteriochromes: Sensors of color and power. *Biochemistry* 51(48):9667-9677.
15. Rockwell NC, Martin SS, & Lagarias JC (2012) Mechanistic insight into the photosensory versatility of DXCF cyanobacteriochromes. *Biochemistry* 51(17):3576-3585.
16. Hirose Y, *et al.* (2013) Green/red cyanobacteriochromes regulate complementary chromatic acclimation via a protochromic photocycle. *Proc Natl Acad Sci USA* 110(13):4974-4979.
17. Rockwell NC, Martin SS, & Lagarias JC (2016) Identification of cyanobacteriochromes detecting far-red light. *Biochemistry* 55(28):3907-3919.
18. Fushimi K, *et al.* (2019) Rational conversion of chromophore selectivity of cyanobacteriochromes to accept mammalian intrinsic biliverdin. *Proc Natl Acad Sci USA* 116(17):8301-8309.
19. Frankenberg N & Lagarias JC (2003) Phycocyanobilin:ferredoxin oxidoreductase of *Anabaena* sp. PCC 7120. Biochemical and spectroscopic characterization. *J Biol Chem* 278(11):9219-9226.
20. Narikawa R, *et al.* (2015) A biliverdin-binding cyanobacteriochrome from the chlorophyll d-bearing cyanobacterium *Acaryochloris marina*. *Sci Rep* 5:7950.
21. Fushimi K, *et al.* (2016) Photoconversion and fluorescence properties of a red/green-type cyanobacteriochrome AM1_C0023g2 That Binds Not Only Phycocyanobilin But Also Biliverdin. *Front Microbiol* 7:588.
22. Blain-Hartung M, *et al.* (2018) Cyanobacteriochrome-based photoswitchable adenylyl cyclases (cPACs) for broad spectrum light regulation of cAMP levels in cells. *J Biol Chem* 293(22):8473-8483.
23. Rockwell NC, Martin SS, Gulevich AG, & Lagarias JC (2014) Conserved phenylalanine residues are required for blue-shifting of cyanobacteriochrome photoproducts. *Biochemistry* 53(19):3118-3130.
24. Lim S, *et al.* (2018) Correlating structural and photochemical heterogeneity in cyanobacteriochrome NpR6012g4. *Proc Natl Acad Sci USA* 115(17):4387-4392.